Electronic structures of GaN edge dislocations

Seung Mi Lee, Mohamed Akli Belkhir,* Xiao Yan Zhu, and Young Hee Lee†
Department of Semiconductor Science and Technology, and Semiconductor Physics Research Center, Jeonbuk National University, Jeonju 561-756, Korea

Yong Gyoo Hwang
Department of Physics, Wonkwang University, Iksan 570-749, Korea

Thomas Frauenheim
Universität-GH Paderborn, Fachbereich Physik, Theoretische Physik, 33095 Paderborn, Germany
(Received 6 January 2000)

We investigate atomic and electronic structures of the threading edge dislocations of GaN using self-consistent-charge density-functional tight-binding approaches. Full-core, open-core, Ga-vacancy, and N-vacancy edge dislocations are fully relaxed in our total-energy scheme. The Ga-vacancy dislocation is the most stable in a wide range of Ga chemical potentials, whereas full-core and open-core dislocations are more stable than others in the Ga-rich region. Partial dehybridization takes place during the lattice relaxation near the dislocation in all cases. The dangling bonds at Ga atoms mostly contribute to the deep-gap states, whereas those at N atoms contribute to the valence-band tails. All the edge dislocations can act as deep trap centers, except the Ga-vacancy dislocation, which may act as an origin of yellow luminescence.

I. INTRODUCTION

Gallium nitride has been suggested as the most promising material for optoelectronic devices. The wide band gap of GaN (3.4 eV) opens applications for a light-emitting diode, covering from green to ultraviolet regions,[1] and a blue laser diode.[2] However, a broad luminescence centered at 2.2–2.3 eV, the so-called yellow luminescence (YL), has been observed under most experimental growth conditions.[3–6] The origin of YL and even the positions of transitions are still being debated. It has been controversial whether YL is due to native defects[5–7] or to impurities.[8–10] It has been observed that the intensity of YL increases with the concentration of the Ga vacancy, particularly in *n*-type GaN,[11] and furthermore the Ga vacancy is energetically the most favorable configuration in *n*-type GaN.[12] However, the Ga vacancy itself is a shallow accepter,[12] and hence the Ga-vacancy/impurity complex has been suggested to be one of the sources as YL.[3,10] Transitions between a shallow donor and a deep acceptor[13] or a deep donor and a shallow acceptor[14] could be responsible for YL. Although the origin of YL from point defects is still unclear, we focus in this work on the possibility that the threading edge dislocation is a source of the YL.

The effect of dislocations on GaN optical properties is still not well understood. One puzzle among several others is that efficient optical devices such as blue-light-emitting diodes can be realized with GaN systems despite the presence of a high density ($\sim 10^{10}$ cm^{-2}) of threading dislocations, while a dislocation density of 10^4 cm^{-2} is usually sufficient to prevent laser operation in GaAs-based optical emitters.[1,15–17] On the other hand, there is experimental evidence that dislocations act as nonradiative recombination centers by cathodoluminescence,[18–20] and also act as electron scattering centers.[21,22] It has been suggested that YL could be related to threading dislocations with a screw component.[23] Recent theoretical calculations[24,25] indicated that dislocations may well be charged, giving rise to deep-gap states. However, other investigations[26] showed that threading edge dislocations and screw dislocations do not contribute to gap states, and hence do not act as nonradiative recombination centers. It is still not clear whether pure dislocations, not compounded with impurities, are responsible for YL. Additional systematic studies are required for pure dislocations.

In this paper, we explore deep-gap states, via the electronic local density of states, related atomic geometries, and stabilities of various edge dislocations, using a self-consistent-charge density-functional-based tight-binding (SCC-DFTB) approach.[27,28] We will demonstrate that the edge dislocations themselves can contribute to YL even in the absence of impurities in GaN. The formation energy calculations of dislocations show that open- and full-core dislocations are favored in Ga-rich conditions, whereas the Ga-vacancy dislocation is the most stable configuration in a wide range of Ga chemical potentials. Pair-correlation functions show that lattices are distorted locally up to the second-nearest neighbor near dislocations. Dehybridization takes place so as to enhance sp^2+p bondings, as seen in bond-angle distribution functions. The dangling bonds at Ga and N atoms mostly contribute to deep-gap states and valence-band tails, respectively. All the edge dislocations can act as deep-trap centers except the Ga-vacancy dislocation, which may act as an origin for YL. Full- and open-core dislocations show deep-gap states which are mostly contributed by the Ga dangling bonds located at the dislocation.

II. THEORETICAL DETAILS

Studying atomic and electronic structures of dislocations requires a large-sized supercell, and they are computationally

0163-1829/2000/61(23)/16033(7)/$15.00 PRB 61 ©2000 The American Physical Society

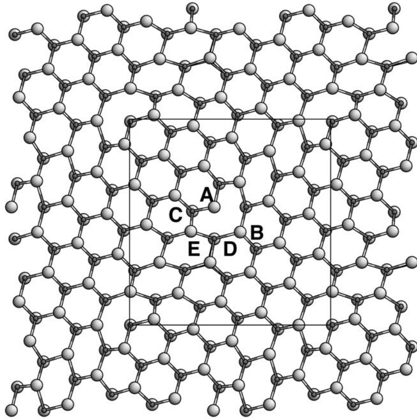

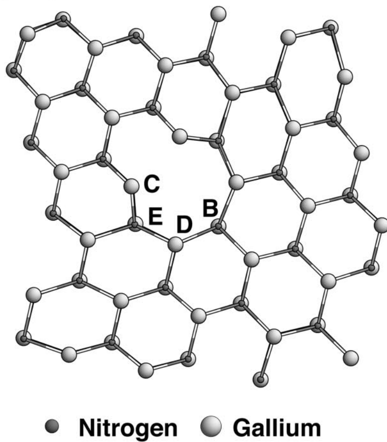

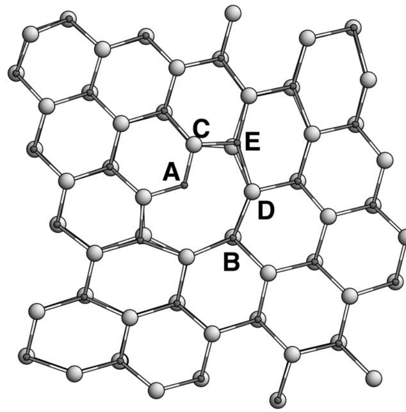

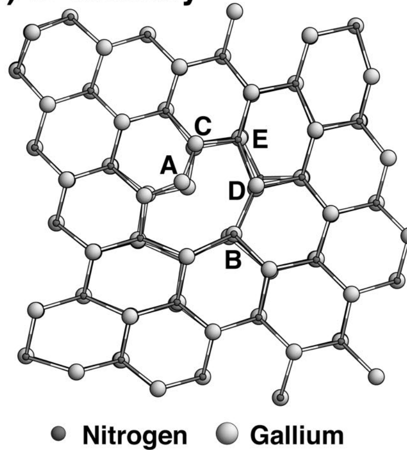

FIG. 1. The fully relaxed geometries of (a) full-core, (b) open-core, (c) Ga-vacancy, and (d) N-vacancy edge dislocations. The bright large ball and the dark small ball represent Ga and N atoms, respectively. The box in (a) shows the size of supercell used in this study. The heavily distorted atoms are identified as A–E.

expensive and often inaccessible with first-principles calculations. In this study, we adopt an efficient SCC-DFTB approach for total-energy calculations. The SCC-DFTB method uses a basis of numerically described s, p, and d atomic orbitals. Hamiltonian and overlap matrix elements were evaluated by a two-center approach. Charge transfer is taken into account through the incorporation of a self-consistency scheme for Mulliken charges based on a second-order expansion of the Kohn-Sham energy in terms of charge-density fluctuations. The diagonal elements of the Hamiltonian matrix employed are then modified by charge-dependent contributions in order to describe the change in the atomic potentials due to the charge transfer. The off-diagonal elements have additional charge-dependent terms due to the Coulomb potential of the ions. They decay as $1/r$, and thus account for the Madelung energy of the system. We emphasize that an accurate description of charge transfer is particularly necessary for systems with a strong ionic bonding character. This method was applied to many different systems of GaN.[26,29–32] Further details of the SCC-DFTB method were published elsewhere.[28]

We first chose a supercell of 224 atoms $(2\sqrt{3}a\times 7a \times 2c)$ for ideal wurtzite GaN. The calculated lattice parameters are $a=3.178$ Å and $c=5.214$ Å, in good agreement within errors values of less than 1 ($a=3.189$ Å,$c=5.185$ Å). The calculated bulk modulus is 189 GPa, comparable to 195 GPa of the measured value.[33] A considerable amount of electron charge $(0.56e)$ is transferred from Ga to N, resulting in an ionic bonding nature. N loses some s electrons and gains more p electrons, whereas Ga loses more p electrons than s electrons. The calculated band gap is 6.52 eV,[34] overestimated by 3.1 eV compared with the observed value of 3.42 eV.

III. RESULTS AND DISCUSSION

We construct a supercell with two edge dislocations by slightly displacing two sets of supercells with each other. Dangling bonds are located in edge dislocations along the line of the [0001] direction. Figure 1(a) shows the fully relaxed geometry of a full-core edge dislocation. The small dark balls represent N atoms, while the large bright balls represent Ga atoms. An open-core dislocation is created by removing a column of Ga and N atoms at the A site from Fig. 1(a), as shown in Fig. 1(b). Nonstoichiometric Ga and N-vacancy dislocations are also constructed by removing a column of Ga and N atoms at the A site, respectively, as shown in Figs. 1(c) and 1(d). Note that the supercell contains two edge dislocations of opposite signs in order to maintain a periodicity perpendicular to the [0001] direction of the dislocation line. The energies of each configuration are minimized using the steepest-descent method, until the maximum

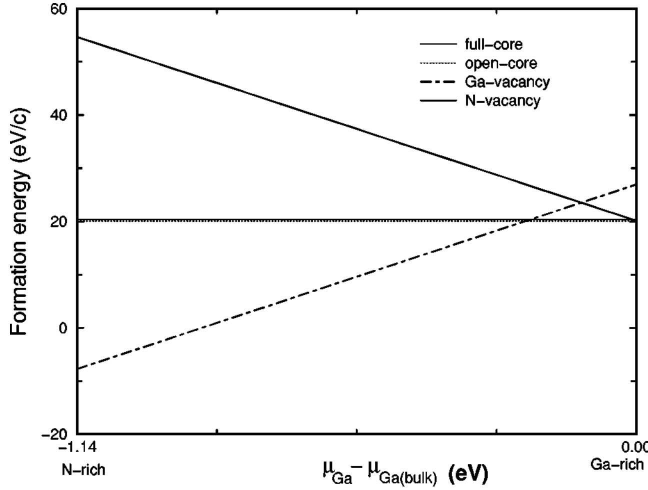

FIG. 2. The formations energies of four dislocations depending on the Ga chemical potential μ_{Ga}. The formations energies are in units of eV per unit c-axis length 5.214 Å.

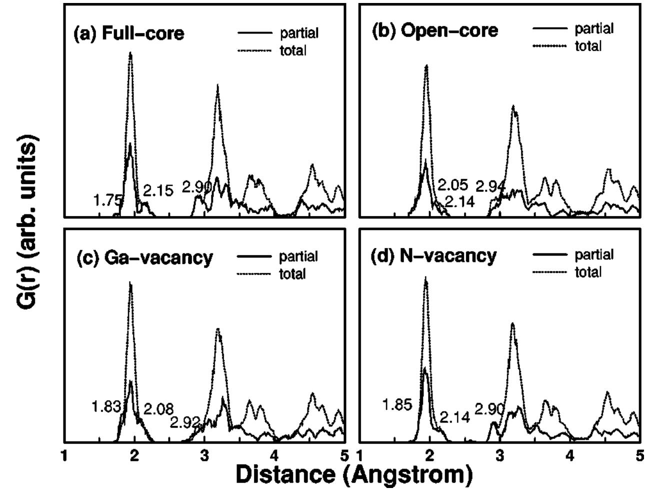

FIG. 3. The PCF's of (a) full-core, (b) open-core, (c) Ga-vacancy, and (d) N-vacancy dislocations. The dotted lines indicate PCF's from all atoms in each geometry, while the solid lines indicate those from the atoms of A–E sites to the first-nearest-neighbor atoms of them. The numbers indicate the PCF peak positions originated from the dislocations.

forces on each atom are less than 0.001 a.u.

We first calculate the formation energies of each configuration in order to test the relative stability. The formation energy can be calculated by

$$E_{form} = E_{total} - n_{Ga}\mu_{Ga} - n_N\mu_N = E_{total} - \mu_{GaN(bulk)} n_N - \mu_{Ga}(n_{Ga} - n_N), \qquad (1)$$

where E_{total} is the total energy of each geometry, $\mu_{GaN(bulk)}$ is the chemical potential of the bulk GaN, and n_{Ga} and n_N represent the number of Ga and N atoms in a supercell, respectively. μ_{Ga} and μ_N are dependent quantities in a GaN system, through the relationship $\mu_{GaN} = \mu_{Ga} + \mu_N$. The second equation is extracted using this equation. μ_{Ga}, the chemical potential of Ga, is under the restriction $\mu_{Ga(bulk)} - \Delta H_f \leq \mu_{Ga} \leq \mu_{Ga(bulk)}$. We used -1.14 eV for ΔH_f, the heat of formation of GaN. The chemical potential of bulk GaN was -294.26 eV, which was obtained by dividing the total energy of bulk GaN by the number of GaN pairs. We used an orthorhombic bulk Ga (Ref. 35) for μ_{Ga} (-224.15 eV) as a reference for the Ga-rich condition. This means that μ_{Ga} cannot exceed the value of an orthorhombic bulk system. The formation energies as a function of μ_{Ga} are shown in Fig. 2. It is clear that the Ga-vacancy dislocation is the most favorable among others in a wide range of N-rich conditions: $-1.14 \leq \mu_{Ga} - \mu_{Ga(bulk)} \leq 0.21$. This is consistent with previous calculation.[24] Open- as well as full-core dislocations become more favorable near the Ga-rich region. In an extreme case of a Ga-rich condition, the N-vacancy dislocation is also an energetically favorable configuration, as suggested in previous calculations.[24] The growth occurs under Ga-rich conditions because of the very high nitrogen equilibrium pressure at a given growth temperature.[7]

Figure 3 shows pair-correlation functions (PCF's) of four dislocation geometries. The solid lines indicate partial PCF's near the dislocations, from the atoms at the A site to the E site only, and the dotted lines indicate those from total atomic configurations. It is clearly shown that the peaks become broader in the first- and second-nearest-neighbors positions due to the dislocations. The numbers in figures indicate the peak positions from the distorted atoms. Bond lengths with atoms at the A site become shorter, compared to the ideal bond length of 1.95 Å, while those with atoms at the B site are enlarged in all cases, resulting in outward relaxations. The bond lengths near A and C sites become shorter, whereas those near B and D sites are extended. The detailed information is summarized in Table I. The bond lengths are relatively widely distributed near the D site in full-core dislocations, and even more widely distributed near D and E sites in open-core dislocations. In Ga-vacancy dislocations, the B site as well as the E site show a wide distribution of bond lengths, whereas B and D sites show wide bond length distributions in N-vacancy dislocations. The N-vacancy dislocation induces the most severe lattice distortions among others, particularly at B and D sites, as also shown in Fig. 1(d). It could be suggested that the electron charges of Ga atoms at the A site are lacking due to the

TABLE I. The average bond lengths with standard deviations in Å around each site at the edge dislocation.

Type	A site	B site	C site	D site	E site
full core	1.84 ± 0.0	2.17 ± 0.05	1.88 ± 0.04	2.03 ± 0.09	1.94 ± 0.05
open core		2.07 ± 0.02	1.82 ± 0.03	2.03 ± 0.32	2.03 ± 0.16
Ga vacancy	1.84 ± 0.0	2.08 ± 0.25	1.85 ± 0.04	2.04 ± 0.06	1.99 ± 0.11
N vacancy	1.88 ± 0.04	2.26 ± 0.23	1.89 ± 0.03	2.13 ± 0.21	1.98 ± 0.08

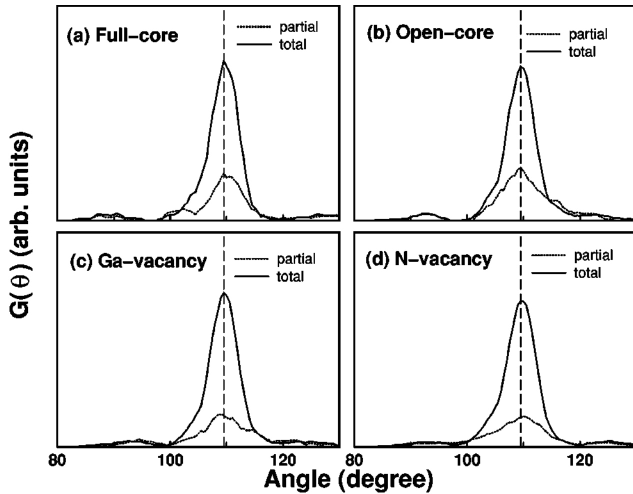

FIG. 4. The BADF's of (a) full-core, (b) open-core, (c) Ga-vacancy, and (d) N-vacancy dislocations. The solid lines indicate BADF's from all atoms in each geometry, while the dotted lines indicate those centered at A–E sites.

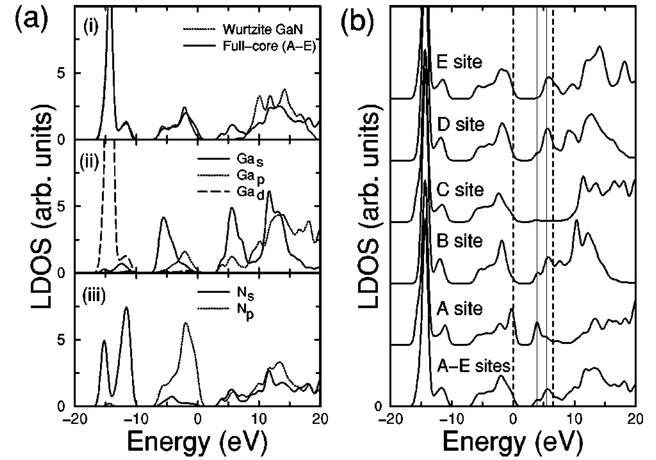

FIG. 5. The LDOS of the full core projected to the heavily distorted atoms at A–E sites. (a) (i) total LDOS (solid line) and that of pure wurtzite GaN (dotted line), (ii) LDOS of s (solid line), p (dotted), and d orbitals (dashed line) of Ga atoms, and (iii) LDOS of s (solid), and p orbitals (dotted) of N atoms. (b) LDOS's of A–E sites, A, B, C, D, and E sites from the bottom. The dashed lines show the band gap of pure wurtzite GaN. The thin solid lines along LDOS axis represent relatively strong gap states.

stronger electronegativity of nitrogen atoms, resulting in stronger ionic repulsive forces between Ga atoms at the dislocation sites and thus inducing symmetry breaking. We expect severe lattice distortions to induce several deep-gap states, as will be discussed in the next paragraph.

The bond angle distribution functions (BADF's) are shown in Fig. 4. The broad peaks near 90° and 120°, originated from atoms at mostly B, D, and E sites in all dislocations, exist in addition to the main peak at 109.5° from bulk structure. The bond angles near 90° and 120° show p^3- and sp^2-like characteristics, respectively. Thus the total energy is minimized by dehybridizing the unpaired electrons of undercoordinated atoms and the electrons of the severely distorted atoms near the dislocation sites. The energy minimization by dehybridization usually occurs in covalent bonding materials with undercoordinated atoms.[36,37] The degree of dehybridization determines the position of gap states, which will be discussed in a later paragraph. The bond angles for each dislocation site are listed in Table II.

The density of states (DOS) is calculated to investigate the electronic structure of dislocations. The local DOS (LDOS) is calculated by projecting the density of states to specific orbitals of a given atom. Figure 5(a) shows the LDOS of the full-core configuration. The solid line in Fig. 5(a)(i) indicates the LDOS of atoms at A–E sites in the full-core dislocation, and the dotted line indicates the DOS of wurtzite GaN for comparison. It is clearly shown that several states exist in the gap due to the dislocations. Figures 5(a)(i) and 5(a)(ii) show the LDOS of each orbital of Ga and N atoms only, respectively. The subscripts represent the specified orbitals in each figure. The s orbitals of Ga atoms mostly contribute to the relatively deep unoccupied states, whereas the p orbitals of Ga atoms contribute both the valance-band tails and gap states. The d orbitals do not contribute to the gap states. Figure 5(a)(iii) also shows that the s orbitals of N atoms contribute mostly to the unoccupied deep states, whereas the p orbitals mostly contribute to the valence band tails.

We further calculate the LDOS of each specific atom one by one, to identify the origin of gap states, as shown Fig. 5(b). The dotted lines indicate the width of band gap of wurtzite GaN, and the solid lines indicate the peak positions of gap states. Our calculated band gap is 6.52 eV, overestimated by 3.1 eV, compared with that of the experimental value for wurtzite GaN. In all theoretical approaches including density-functional theories with local-density approximations, the unoccupied states are poorly described, giving rise to either an overestimation or underestimation of the energy gap. More elaborate approaches with GW approximations will give more accurate descriptions of the band gap.[38] The overestimation of the band gap may be corrected by several approximations. The simplest one, which is usually adopted in most wide-band-gap materials, is the scissors operation, which simply shifts the unoccupied states to fit to the experimental values. However, it is not so simple in a case where

TABLE II. The average bond angles with standard deviations in degree centered at each site of the edge dislocation.

Type	A site	B site	C site	D site	E site
full core	108.5±0.6	110.4±8.6	105.4±4.1	110.8±15.9	107.0±17.6
open core		110.2±8.0	114.7±0.2	109.1±12.0	106.9±13.3
Ga vacancy	101.7±0.1	101.7±6.8	107.0±6.5	109.6±13.0	107.2±12.5
N vacancy	99.4±2	110.8±11.6	106.1±4.9	109.4±11.5	108.8±11.9

TABLE III. The position of gap states from the valence-band top in eV localized at each site of the edge dislocation. The values are obtained by the linear scaling method.

Type	*A* site	*B* site	*C* site	*D* site	*E* site
full core	2.0	2.1	2.0	2.1	3.0
	2.7	3.0		2.9	
open core		3.0	1.4		1.4
Ga vacancy	0.2	3.1		3.2	
	3.2				
N vacancy	1.4	0.6	1.3	0.6	2.8
	2.2	1.9	2.2	2.6	
	3.1	2.9	3.0		

gap states are involved. In our approach, we adopt a linear scaling method, similar to what was done in previous studies.[39] All energy levels in the gap are projected to the valence and conduction bands of bulk GaN. The energy levels are then presumably shifted downwards by the fraction of the band-gap correction. The values after the scaling are listed in Table III.

Figure 5(b) clearly shows that the deep-gap (unoccupied) states centered at $E_{VB}+2.1$ eV originate from the *s* and *p* orbitals of Ga atoms at *A* and *B* sites, where E_{VB} is the energy level of the top valence band. A more prominent peak near $E_{VB}+2.9$ eV also appears in the full-core dislocation, originating mostly from the *s* orbitals of the Ga and *p* orbitals of N atoms at *B*, *D*, and *E* sites. The valence-band tails are mostly contributed from the N atoms at the *A* site. This situation is similar to the previous calculations, where valence-band states are mostly localized on threefold N sites in amorphous GaN.[40]

For the open-core dislocation, deep-gap (unoccupied) states exist around $E_{VB}+1.4$ eV, as shown in Fig. 6, mostly originating from the *s* and *p* orbitals of Ga atoms and the *p* orbitals of N atoms. The valence-band tails are mostly contributed from the *p* orbitals of Ga and N atoms, while the conduction-band tails are mostly contributed from the *s* orbitals of Ga and N atoms. The deep-gap states at E_{VB}

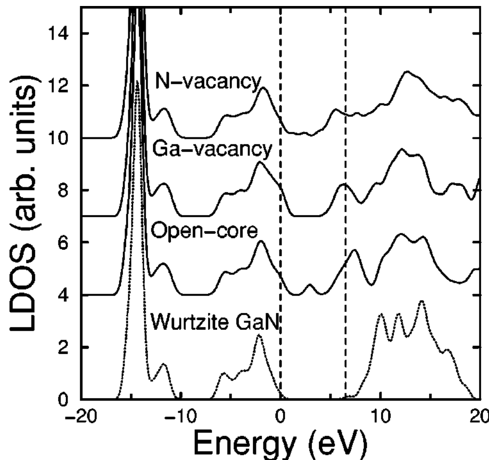

FIG. 6. The LDOS of the heavily distorted atoms at *A* to *E* sites for open-core, Ga-vacancy, and N-vacancy dislocations. The DOS for wurtzite GaN is also shown for comparison. The dashed lines show the band gap of pure wurtzite GaN.

$+1.4$ eV is attributed mostly to the *s* and *p* orbitals of Ga atoms at the *C* site, and slightly from the Ga atoms at the *E* site. This may act as a trap center for radiative transitions (for instance, for YL) from the conduction bands. This will be discussed more in detail in a later paragraph. The *s* orbitals of Ga atoms at the *B* site contribute to the shoulder around the conduction-band tails at $E_{VB}+3.0$ eV.

No deep gap states are found in the Ga-vacancy dislocation, as shown in Fig. 6. This is similar to the point defect of the Ga-vacancy dislocation in GaN, where the gallium vacancy is a shallow acceptor.[12,41] The conduction-band tails are contributed from the *s* orbitals of Ga and N atoms. The *p* orbitals of N atoms mostly contribute to the valence-band tails. It is worth noting that the Ga-vacancy dislocation contribute the most shallow levels among the dislocations. Shallow levels exist at 0.2 eV from the bottom of the conduction bands and the top of the valence band, respectively. We note that only N atoms are located at the *A* site in this case. N atoms will have more excessive charges due to the stronger electronegativity. All these electrons contribute to the valence-band tails as occupied states, consistent with those from amorphous GaN.[40] The lattice relaxations induced by these excessive electrons will occur so as to maximize the dehybridization, pushing the deep-gap states toward the band tails. This can be confirmed from the BADF shown in Fig. 4(c). Shallow unoccupied gap states at $E_{VB}+3.2$ eV or $E_{CB}-0.2$ eV originate from the *s* orbital of the Ga atom at *B* and *D* sites.

The N vacancy induces several gap states at the dislocations which are spread over the wide range of energy gap from both Ga and N atoms, as shown in Fig. 6. The peak at $E_{VB}+0.6$ eV is contributed from *B* and *D* sites as occupied states. In this geometry, we have Ga atoms only at the *A* site. Since the excessive charges of Ga atoms at the *A* site are depleted to the adjacent N atoms due to the smaller electronegativity, screening effects are diminished. Increased repulsive forces between Ga ions will result in severe lattice distortions, as shown in Fig. 1(d). However, the dehybridization of electrons at the Ga atoms occurs less severely, such that several deep-gap states are spread about. Less prominent peaks at similar positions are also shown in other sites. Detailed values are listed in Table III.

So far we have discussed the positions of gap states of each configuration. Figure 7 shows a schematic diagram to show the energy levels in the gap for each configuration. Full- and open-core dislocations have deep-gap states at $E_{VB}+2.0$ eV and $E_{VB}+1.4$ eV, respectively, which may act as deep acceptors and play as YL centers. Full-core dislocations will have YL for a transition from a level around 2.0 eV to the valence band. This level may be identified by photoluminescence excitation measurements. It will also play a role for nonradiative recombination centers which involve transitions from conduction-band-edge states to levels above 2.0 eV. Open-core dislocations will also play a role for the YL center, involving a transition from the conduction-band edge to the level at $E_{VB}+1.4$ eV. The Ga-vacancy dislocation has shallow levels within 0.2 eV from the band edges. Several gap states are widely spread over the entire energy gap in case of N-vacancy dislocations. In Ga-rich conditions, all configurations except Ga-vacancy dislocations are energetically favorable, as shown in Fig. 2. We therefore believe

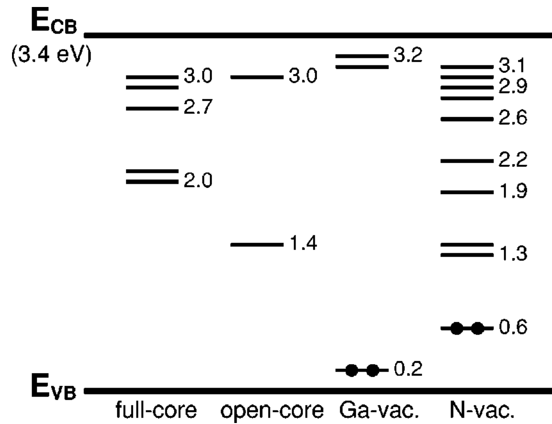

FIG. 7. The schematic diagram of energy levels in the band gap for each edge dislocation. Filled circles indicate occupied states.

that full-core, open-core, and N-vacancy dislocations should exist in Ga-rich conditions, which is an experimentally favorable situation.[7] It is very likely that these configurations will play roles for the YL centers. Since the N-vacancy dislocation has several gap states over the entire range of energy gaps, this involves not only the YL center but also nonradiative recombination centers. We conclude that pure dislocations can contribute to the YL center as well as to nonradiative recombination centers. A possibility for the dislocations to be associated with impurities such as oxygens or silicons cannot be excluded, as discussed in the previous calculations.[29]

IV. SUMMARY

In summary, we performed SCC-DFTB calculations to elucidate the electronic structure of edge dislocations in wurtzite GaN. We find that full-core, open-core, and N-vacancy dislocations are favorable in Ga-rich conditions, whereas the Ga-vacancy dislocation is the most favorable in a wide range of N-rich conditions. Several unoccupied gap states exist in all cases. The *s* and *p* orbitals of Ga atoms mostly contribute to the gap states, while N atoms contribute to the valence-band tail in most cases. We conclude that edge dislocations can act as trap centers for electrons and contribute to the YL center, except the Ga-vacancy dislocation at the core of the edge dislocation.

ACKNOWLEDGMENTS

We acknowledge the financial support by the Korea Science and Engineering Foundation (KOSEF) and in part by BK21 program. One of us (T.F.), acknowledges the financial support from the Deutsche Forschungsgemeinschaft.

*Present address: Department of Physics, University of Bejaia, Bejaia 06000, Algerie.
†Author to whom correspondence should be addressed. Electronic address: leeyh@sprc2.chonbuk.ac.kr. Also at Department of Physics, Jeonbuk Nat'l Univ., Jeonju, 561-756.

[1] S. Nakamura, T. Mukai, and M. Senoh, J. Appl. Phys. **76**, 8189 (1994).
[2] S. Nakamura, M. Senoh, S. Nagahama, N. Iwsa, T. Yamada, T. Matsushita, H. Kiyoku, and Y. Sugimoto, Jpn. J. Appl. Phys. **35**, L74 (1996).
[3] F.A. Ponce, D.P. Bour, W. Götz, and P.J. Wright, Appl. Phys. Lett. **68**, 57 (1996).
[4] T. Suski, P. Berlin, H. Teisseyre, M. Leszcynsky, I. Grzegory, J. Jun, M. Bockowski, S. Porowski, and T.D. Moustakas, Appl. Phys. Lett. **67**, 2188 (1995).
[5] L.W. Tu, Y.C. Lee, S.J. Chen, I. Lo, D. Stocker, and E.F. Schubert, Appl. Phys. Lett. **73**, 2802 (1998).
[6] H. Siegle, P. Thurian, L. Eckey, A. Hoffmann, C. Thomsen, B.K. Meyer, H. Amano, I. Akasaki, T. Detchprohm, and K. Hiramatsu, Appl. Phys. Lett. **68**, 1265 (1996).
[7] P. Perlin, T. Suski, H. Teisseyre, M. Leszczynski, I. Grzegory, J. Jun, S. Porowski, P. Boguslawski, J. Bernholc, J.C. Chervin, A. Polian, and T.D. Moustakas, Phys. Rev. Lett. **75**, 296 (1995).
[8] C. Wetzel, T. Suski, J.W. Ager III, E.R. Weber, E.E. Haller, S. Fischer, B.K. Meyer, and P. Perlin, Phys. Rev. Lett. **78**, 3923 (1997).
[9] C.G. Van de Walle and J. Neugebauer, Mater. Sci. Forum **258-263**, 19 (1997).
[10] J. Neugebauer and C.G. Van de Walle, Appl. Phys. Lett. **69**, 503 (1996).
[11] K. Saarinen, T. Laine, S. Kuisma, J. Nissilä, P. Hautojärvi, L. Dobrzynski, J.M. Baranowski, K. Pakula, R. Stepniewski, M. Wojdak, A. Wysmolek, T. Suski, M. Leszczynski, I. Grzegory, and S. Porowski, Phys. Rev. Lett. **79**, 3030 (1997).
[12] J. Neugebauer and C.G. Van de Walle, Phys. Rev. B **50**, 8067 (1994).
[13] T. Ogino and M. Aoki, J. Appl. Phys. **19**, 2395 (1980).
[14] E.R. Glaser, T.A. Kennedy, K. Doverspike, L.B. Rowland, D.K. Gaskill, J.A. Freitas, Jr., M.A. Khan, D.T. Oslon, J.N. Kunznia, and D.K. Wickenden, Phys. Rev. B **51**, 13 326 (1995).
[15] F.A. Ponce, MRS Bull. **22**, 51 (1997).
[16] F.A. Ponce, D. Cherns, W.T. Young, and J.W. Steeds, Appl. Phys. Lett. **69**, 770 (1996).
[17] S.D. Lester, F.A. Ponce, M.G. Cranford, and D.A. Steigetwald, Appl. Phys. Lett. **66**, 1249 (1996).
[18] S.J. Rosner, E.C. Carr, M.J. Ludowise, G. Girlami, and H.I. Erikson, Appl. Phys. Lett. **70**, 420 (1997).
[19] T. Sugahara, H. Sata, M. Hao, Y. Naoi, S. Kurai, S. Tottori, K. Yamashita, K. Nishino, L.T. Romano, and S. Sakai, Jpn. J. Appl. Phys. **37**, L398 (1998).
[20] F.A. Ponce, D.P. Bour, and W. Götz, Appl. Phys. Lett. **68**, 57 (1996).
[21] H.M. Ng, D. Doppalapudi, T.D. Moustakas, N.G. Weimann, and L.F. Eastman, Appl. Phys. Lett. **73**, 821 (1998).
[22] N.G. Weimann, L.F. Eastman, D. Doppalapudi, H.M. Ng, and T.D. Moustakas, J. Appl. Phys. **83**, 3656 (1998).
[23] S. Christiansen, M. Albrecht, W. Dorsch, H.P. Strunk, C. Zanotti-Fregonara, G. Salviati, A. Pelzmann, M. Mayer, M. Kamp, and K.J. Ebeling, MRS Internet J. Nitride Semicond. Res. **1**, 19 (1996).
[24] A.F. Wright and U. Grossner, Appl. Phys. Lett. **73**, 2751 (1998).
[25] D.C. Look and J.R. Sizelove, Appl. Phys. Lett. **82**, 1237 (1999).
[26] J. Elsner, R. Jones, P.K. Sitch, V.D. Porezag, M. Elstner, Th. Frauenheim, M.I. Heggie, S. Öberg, and P.R. Briddon, Phys. Rev. Lett. **79**, 3672 (1997).
[27] D. Porezag, Th. Frauenheim, and Th. Köhler, Phys. Rev. B **51**, 12 947 (1995).

[28] M. Elstner, D. Porezag, G. Jungnickel, J. Elsner, M. Haugk, Th. Frauenheim, S. Suhai, and G. Geifert, Phys. Rev. B **58**, 7260 (1998).

[29] J. Elsner, R. Jones, M.I. Heggie, P.K. Sitch, M. Haugk, Th. Frauenheim, S. Öberg, and P.R. Briddon, Phys. Rev. B **58**, 12 571 (1998).

[30] S.M. Lee, Y.H. Lee, Y.G. Hwang, J. Elsner, D. Porezag, and Th. Frauenheim, Phys. Rev. B **60**, 7788 (1999).

[31] S.M. Lee, Y.H. Lee, Y.G. Hwang, J. Joachim, and T. Frauenheim, MRS Internet J. Nitride Semicond. Res. **4S1**, G6.3 (1999).

[32] S.M. Lee, Y.H. Lee, Y.G. Hwang, and C.J. Lee, J. Korean Phys. Soc. **34**, S253 (1999).

[33] K. Miwa and A. Fukumoto, Phys. Rev. B **48**, 7897 (1993).

[34] We checked the supercell size dependence of band gap. Doubling the supercell along *c*-axis increases band gap by 0.02 eV, which was negligible.

[35] R.W.G. Wylckoff, *Crystal Structures*, 2nd ed. (John Wiley & Sons, New York, 1964), Vol. 2, Chap. 2.

[36] S.M. Lee and Y.H. Lee, Surf. Sci. **347**, 329 (1996).

[37] E. Kim and Y.H. Lee, Phys. Rev. B **50**, 5429 (1995).

[38] A. Rubio, J.L. Corkill, M.L. Cohen, E.L. Shirley, and S.G. Louie, Phys. Rev. B **48**, 11 810 (1993).

[39] P. Boguslawski, E.L. Briggs, and J. Bernholc, Phys. Rev. B **51**, 17 255 (1995).

[40] P. Stumm and D.A. Drabold, Phys. Rev. Lett. **79**, 677 (1997).

[41] D.W. Jenkins and J.D. Dow, Phys. Rev. B **39**, 3317 (1989).